



# Sono-sorption efficiencies and equilibrium removal of triphenylmethane (crystal violet) dye from aqueous solution by activated charcoal

Sobhy M. Yakout <sup>a, b</sup>, Mohamed R. Hassan <sup>c, \*</sup>, Ahmed A. Abdeltawab <sup>d, e</sup>, Mohamed I. Aly <sup>b</sup>

<sup>a</sup> Department of Biochemistry, College of Science, King Saud University, Riyadh, 11451, Saudi Arabia

<sup>b</sup> Department of Analytical Chemistry and Control, Hot Laboratories and Waste Management Center, Atomic Energy Authority, Cairo, 13759, Egypt

<sup>c</sup> Nuclear Research Center, Atomic Energy Authority, P.O. 13759, Inshas, Cairo, Egypt

<sup>d</sup> Department of Chemistry, College of Science, King Saud University, Riyadh, 11451, Saudi Arabia

<sup>e</sup> Tabbin Institute for Metallurgical Studies, Cairo, Egypt

## ARTICLE INFO

### Article history:

Received 17 March 2019

Received in revised form

24 May 2019

Accepted 15 June 2019

Available online 21 June 2019

Handling Editor: Panos Seferlis

### Keywords:

Ultrasound

Sorption

Sonosorption

Crystal violet

Equilibrium

## ABSTRACT

In this present work, the sorption of crystal violet (CV) pigment from laden aqueous solution carried out via ultrasound-assisted. The sorption of CV on activated charcoal was performed in the existence and absence of ultrasound. Using of combined ultrasound/activated charcoal process gave high CV decolorization than using sorption or sonolysis alone because of the synergistic process achieved in this combined system. Experiments were performed at different initial pigment concentration and temperature. The sorption isotherms were achieved by the Freundlich, Langmuir, D–R and Temkin isotherm model. The sorption of CV onto activated charcoal demonstrated more suitable for Langmuir than the Freundlich isotherm model. The maximum monolayer sorption capacity was 50.1 mg/g. The thermodynamic parameters, namely the entropy, Gibbs free energy and enthalpy of the CV sorption process were determined. The enthalpy and free energy indicate an exothermic, feasible and spontaneous process. It has been shown that the proposed combined ultrasound/activated charcoal process may be useable in the treatment of pigment solution from textile wastewater.

© 2019 Elsevier Ltd. All rights reserved.

## 1. Introduction

Wastewater effluents discharged from various sorts of enterprises, for the most part, contain several organic toxins and dangerous substances which are destructive to aquatic life. The effluent released from different ventures, for example, paint, textiles, leather, and paper in the industry. dyestuff fabricating are very shaded wastewater which makes serious environmental concerns everywhere throughout the world (Shirsath et al., 2015).

Crystal violet (CV) is an artificial basic cationic pigment, which in aqueous solution makes violet dye, an affiliate of the triphenylmethane classify and it broadly utilized in cloth coloring productions. It uses for treatment dermatology problems, biological tint, treatment of animals and preservative to hens nurture to diminish the spread of hurtful bacteria. (Jain et al., 2010). The

cationic pigments are more poisonous than the anionic pigments because these can simply react negatively charged cells membrane shells and can pass into cells and converge in the cytoplasm. The CV is a confirmed effective carcinogen, poisonous to mammalian cells and mitotic toxic.

Subsequently, this pigment are containing wastewater must be treated before being released into the getting waterway. In a request to release pigments from wastewater different treatment forms. For example ozonation (Muthukumar et al., 2004), coagulation (Maroušek et al., 2019), ultrafiltration (Majewska-Nowak et al., 1989), oxidization (Kim et al., 2004), electrochemical (Gupta et al., 2007), photocatalytic degradation (Sun et al., 2010) and sorption (Sun et al., 2010). Amongst of these techniques, sorption has been found to be efficient and inexpensive comparing to other methods for removal of pigments, containing dyes and other colorants owing to cost low, its ease operation, design and insensitivity to toxic various materials.

Activated charcoal (AC) is attractive because of its high efficiency but its high cost of production. It is also cannot be utilized to

\* Corresponding author.

E-mail address: [muhmmmed\\_refait@yahoo.com](mailto:muhmmmed_refait@yahoo.com) (M.R. Hassan).

eliminate heavy metals from a large quantity of real waste because the economic feasibility has to be regarded. Different low-cost sorbents produced from wastes of agricultural as rice husk, orange peel, and coconut shell have been utilized to eliminate the pigments from wastewater effluent (Mardooyan and Braun, 2015). Wastes of agricultural are combined with lignin and cellulose as the main ingredients. It may contain another polar functional group of lignin-containing aldehydes, alcohols, ketones, phenolic, ether and carboxylic group for sorption (Marousek et al., 2014).

Recently, ultrasound has attracted increasing attention in the protection of the environment for the destruction of hazardous pollutants as dyes, chlorinated, aromatic compounds, and hydrocarbons in wastewater. Combination of ultrasound with the biosorption process found to be a promising technique in the elimination of chemical pollutants as dyes (Entezari and Soltani, 2009). Many investigators have examined the effects of ultrasound on the biosorption of organic substances by different biosorbents (Entezari and Bastami, 2008).

Combination of two techniques was reported to be more efficient in the elimination of dyes than their serial combination (Entezari and Keshavarzi, 2001). Mechanical and chemical effects of ultrasound have been attributed to the collapse of microscopic bubbles (Liu et al., 2011). The vibration of ultrasonic decrease liquid films thickness attached to the solid phase, simplify the sorbate species diffusion via the interface, improve the mass transfer and destroying the affinity between sorbate and sorbent (Dastkhooon et al., 2017). The asymmetric collapse of the cavity that near of the solid surface is producing a high-speed jet of liquid. The surface is hitting by strong forces comes from these jets. This procedure causes severe destruction at the point of impact, highly reactive surfaces and produces newly exposed. Furthermore, the energy of ultrasonic could change in equilibrium features of the sorption/desorption system and the equilibrium time of the sorption decreased (Eren, 2012).

Dil et al. (2017) have reported that the synthesis of activated carbon/zinc (II) oxide nanorods for simultaneous sorption of CV utilizing ultrasound power. The effects of different operational parameters including sorbent mass, ultrasonic time and initial CV concentration on the responses were investigated. The experimental kinetic data revealed that both pseudo-second-order and intraparticle diffusion models fitted with sorption of CV. The analysis of experimental equilibrium data by four isotherm models and the results showed that the data fitted well with the Langmuir model with maximum sorption capacity of 81.6 mg/g for CV pigment.

Low et al. (2018) described the evaluation of ultrasound modified peanut husk powder (PHP) at several ultrasound energy levels in CV sorption with different conditions of contact time, initial concentration of CV solution, sorbent dosage and pH was studied and contrasted with ultrasound simultaneous sorption process and the control. The sorption removal percent of indirect ultrasound modified (PHP) has raised 25.78%, 13.64% and 1.5% contrasted with the control, ultrasound simultaneous sorption and direct ultrasound modified sorbent respectively at 60 mg/L of initial CV concentration. Indirectly modified sorbent at 3.5 W has attained the highest sorption removal percent of 94.83% at 300 mg sorbent dose for 3 h and 89.96% at solution pH 8.

Hamza et al. (2018) had published the removal of CV from laden aqueous solution onto Raw Tunisian Smectite Clay by Sono-assisted sorption. Batch sorption experiments were performed to investigate the influence of different factors such as contact time, initial CV concentration, sorbent dose and pH on the Sono-assisted sorption of CV pigment. The pseudo-second-order kinetic model fitted to describe sorption kinetic. Freundlich, Langmuir, Toth, and Langmuir–Freundlich isotherms were described well the CV

equilibrium Sono-assisted sorption process.

In nearly all the previous studies were focused on the impact of low power frequency ultrasound on sorption systems. Nevertheless, the sorption equilibria and temperatures in the existence of high-frequency ultrasound utilizing AC as sorbent has not been examined systematically until now. Our study hypothesis was based on the combination of two techniques (adsorption and ultrasound) was reported to be more efficient in the elimination of dyes. In an economical point of view, the most important factor is the reduction of process time and the high efficiency of pollutant removal under ambient conditions which is attainable in this work. To test this hypothesis, aims of this work are to study the sorption of CV from laden aqueous solution by activated charcoal in the presence and absence of high-frequency ultrasound and to clarify the impact of ultrasound on the equilibrium isotherm. The use of ultrasound in combined with AC to treat wastewater provides an alternative, low-cost, effective and innovative water treatment method. This study is expected to guide researchers during future work in the sorption and sono-degradation of aqueous organic waste.

## 2. Experimental section

### 2.1. Materials

Crystal violet (CV) supplied by Merck was used as an adsorbate. A stock solution of the pigment was set up by dissolving the pigment in twice refined water. The adsorbent used in this work was activated charcoal (AC) was supplied by Sigma-Aldrich. Prior to use, the AC was washed repeatedly with distilled water. At long last, the washed AC was dried in an oven at 383 K to steady weight and put away in a desiccator until utilize.

### 2.2. Apparatus

The ultrasonic emission was completed with hardware working at 40 kHz (Power sonic 405). Waves were transmitted from the base of the standard tip which submerged in the solution. The round and the hollow sonochemical reactor (volume = 125 ml) was temperature controlled by the utilization of a water coat.

### 2.3. Analysis

UV–vis spectrophotometer (Spectramax M5, Molecular Devices, Sunnyvale, CA) was utilized to gauge the concentration of CV pigment. The wavelength of the greatest absorbance ( $\lambda_{\max}$ ) of CV pigment was 590 nm. The existence of each functional groups on the surface of the AC was verified by Fourier transform infrared (FT-IR) spectroscopy (Frontier, PerkinElmer, USA). Using nitrogen sorption and desorption method on Belsorp-mini II (BEL, Japan) was operated by at 77 K. The AC specific surface area and total pore volume were computed using the method of Brunauer-Emmett-Teller (BET).

### 2.4. Experiments

In order to investigate the impacts of different test parameters like pigment primary concentration and temperature on the sorption equilibrium isotherm of CV pigment onto AC under high-intensity ultrasound (200 W), the following procedure was used. In the typical experiment, 50 mL of fixed initial concentration 100 mg/L, 0.1 g AC and pH 7.3 was sonicated at foreordained interims of time by the ultrasonic reactor. The effect of initial dye concentration was studied by preparing CV pigment solutions of various concentrations from 5 to 100 mg/L. The constant temperature was

maintained using an ultrasonic reactor except for the experiments where the effect of temperature was studied (25, 65 and 80 °C). The proportion of CV pigment expulsion was evaluated utilizing the following equation:

$$\text{Removal (\%)} = \frac{C_o - C_e}{C_o} \times 100 \quad (1)$$

Here,  $C_o$  and  $C_e$  are the primary and the equilibrium concentrations of CV pigment (mg/L), individually. Further, the measure of pigment sorbed per unit mass of AC (mg/g) was estimated using the following equation

$$Q_e = \frac{V(C_o - C_e)}{m} \quad (2)$$

where  $V$  is the volume of the pigment solution in L and  $M$  is the mass of dry AC in g.

Due to the ingrained alignment causing from the isotherm models linearization, for example, the non-linear regression Root Mean Square Error (RMSE) equation (3), the Sum of Error Squares (SSE) equation (4) and Chi-Squares ( $X^2$ ) equation (5) the test is done as the standard for evaluation of the fitting quality (Abbas et al., 2018). The mathematical equations can be represented as follows:

$$\text{RMSE} = \sqrt{\frac{1}{n-2} \sum_1^n (Q_{e,\text{exp}} - Q_{e,\text{cal}})^2} \quad (3)$$

$$\text{SSE} = \frac{1}{n} \sum_{n=1}^{\infty} (Q_{e,\text{exp}} - Q_{e,\text{cal}})^2 \quad (4)$$

$$X^2 = \sum_1^n \frac{(Q_{e,\text{exp}} - Q_{e,\text{cal}})^2}{Q_{e,\text{cal}}} \quad (5)$$

Here,  $Q_{e,\text{exp}}$  and  $Q_{e,\text{cal}}$  (mg/g) are the experimental and calculated values of CV uptake and  $n$  is the number of data points. When the RMSE, SSE and  $X^2$  values are small that signifies curve fitting is the better (Harrache et al., 2019).

### 3. Theory

#### 3.1. Sorption isotherm

Sorption equilibrium isotherm is essential in depicting the interactive performance amongst sorbates and sorbent and also is main in the sorption techniques analysis and design. The data is obtained from sorption equilibrium are used in the evaluation of the many isotherm models. In the current examination, the isotherm investigation of CV was led at different (5–100 mg L<sup>-1</sup>) with a consistent measure of sorbent (0.1 g/50 ml) at 25 °C. The Langmuir (Rodrigues et al., 2019), Freundlich (Mullerova et al., 2019), Dubinin–Radushkevich (D–R) (Devi and Mishra, 2019) and Temkin (Rodrigues et al., 2019). These models of isotherm were used in describing the equilibrium sorption data.

$$\text{Langmuir} : \frac{C_e}{Q_e} = \frac{C_e}{Q_{\text{Lan}}} + \frac{1}{k_L Q_{\text{Lan}}} \quad (6)$$

$$\text{Freundlich} : \log Q_e = \log K_F + \frac{1}{n} \log C_e \quad (7)$$

$$\text{Dubinin–Radushkevich (D–R)} : \ln Q_e = \ln Q_m - K_{D-R} \epsilon^2 \quad (8)$$

$$\text{Temkin} : Q_e = \beta \ln K_T - \beta \ln C_e \quad (9)$$

From equation (6),  $Q_{\text{Lan}}$  is the Langmuir monolayer capacity of the sorbent in mg/g and  $K_L$  is the Langmuir binding constant in L/mg and identified with the free energy of sorption.

From equation (7),  $K_F$  and  $n$  are constants related to theoretical sorption capacity in [(mg/g) (L/mg)<sup>1/n</sup>] and intensity of sorbent/sorbate binding in the unit less, respectively.

From equation (8),  $Q_m$  is the theoretical isotherm saturation capacity in mg/g,  $K_{D-R}$  is the D–R constant in mol<sup>2</sup>/kJ<sup>2</sup> and  $\epsilon$  is the Polanyi potential that computed by equation (6).

$$\epsilon = RT \ln \left( \left( 1 + \frac{1}{C_e} \right) \right) \quad (10)$$

Here  $R$  in J/mol K, is the real gas constant and  $T$  in K, is the absolute temperature.

From equation (10),  $K_T$  is Temkin equilibrium binding constant in L/g and  $\beta$  is a constant related to the heat of sorption (KJ/mol).

## 4. Result and discussion

#### 4.1. Surface characterization of AC

The BET surface area and pore volume of AC are computed as 595 m<sup>2</sup>g<sup>-1</sup> and 0.5–2 nm, respectively. As shown in Fig. 1, FT-IR spectrum of AC. The broadband was observed at 3300 and 1090 cm<sup>-1</sup> was assigned to O–H stretching and C–O stretching vibration, respectively (Pathania et al., 2017; Zhao et al., 2018). The peaks that appeared at 1570 and 1455 cm<sup>-1</sup> indicated the presence of stretching of aromatic C=C ring (Cohen-Ofri et al., 2006; Ye et al., 2017). Additionally, a band was observed at 800 cm<sup>-1</sup> corresponded to benzene ring vibrations (Cheng et al., 2012). Finally, It was confirmed that a large number of hydroxyl functional groups present on the surface of AC are bonded to aliphatic and aromatic sites.

#### 4.2. Influence of ultrasound on the sorption process

CV decolorization efficiency was achieved under various experimental conditions that consist of (I) sorption, (II) sonolysis, (III) sonosorption utilizing 50 ml of 100 (mg/L) CV with 0.1 g AC for 1 h and the results are shown in Table 1.

The experimental results showed that the decolorization efficiency (%) for removal CV using a combination of ultrasound/AC is much greater than using ultrasound only. CV pigment concentration decolorized under combined ultrasound/AC process was approximately four times greater than that of the pigment concentration decolorized under sorption by AC only and ultrasound only was inadequate for CV decolorization.

Pigment degradation in the existence of AC is much higher than that of ultrasound only because AC is effected via physical and chemical of sonication (Şayan, 2006). During the sonication was produced the acoustic cavitation (formation and collapse of the cavity). Like collapses of the bubble, very high local pressure and the temperature were yielded in the solution (Thompson and Doraiswamy, 1999). Furthermore, the bubbles asymmetrically collapse in a heterogeneous solution leads to the formation of microjets and shockwaves with high speed on the AC surface. This operation leads to disruption of the sorbent structure and may expose new sites that cause an enhancing of the sorption capacity in the existence of ultrasound via an improvement of mass transfer into the pores.

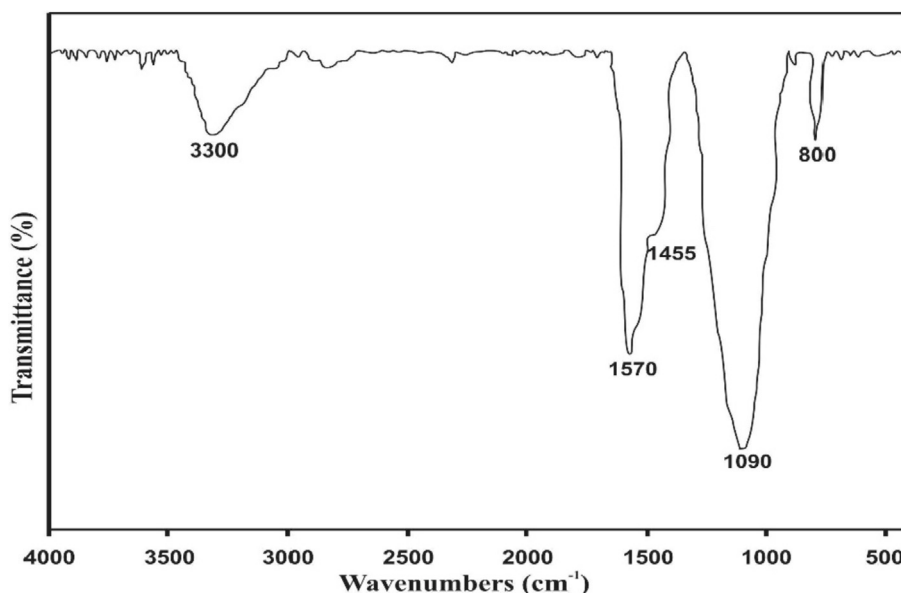


Fig. 1. FTIR spectra of activated charcoal (AC).

Table 1

CV removal under different experimental conditions.

Experimental conditions	Decolorization efficiency (%)
Sorption	12.6
Sonolysis	0.5
Sonosorption	54.4

#### 4.3. Effect of pigment concentration

Effect of initial CV concentrations on biodegradation was investigated to evaluate their capacity to bear various CV concentrations. Sorption trials for the pigment CV were changed in the concentration range of 5–100 mg/L (Fig. 2) with high-frequency ultrasound. The trial results demonstrate that with elevating in initial CV concentration leads to a decrease in the removal percent but AC equilibrium sorption capacity elevate. With elevating the initial pigment concentration elevated from 5 to 100 mg/L, the

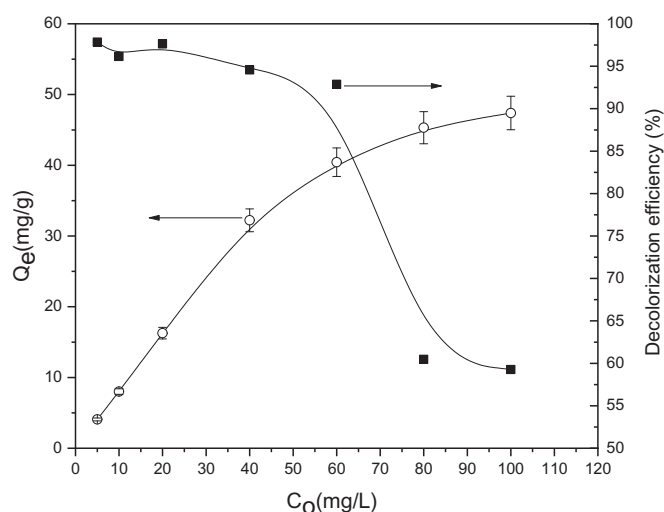


Fig. 2. Impact of initial concentration on the sorption of CV under high-intensity ultrasound.

sorption capacity elevated from 4 to 50 mg/g in the existence of ultrasound but the removal sorption reduced from 98% to 59%. When the concentration above 60 mg/g, the removal percent was high in the existence of ultrasound. Bubbles asymmetric collapse in heterogeneous systems attached to or near the solid boundary that products high-speed jets of liquid and shockwaves are mostly responsible for this enhancement. The main factors for this performance are may be associated to the elevating of the surface area of the solid boundary from decrease induced particle size of the cavitation and enhance of mass transport of solute to the solid surface by acoustic flowing.

#### 4.4. Sorption isotherm

The sorption isotherm can describe the spreading of sorption molecules between the solid and fluid phase when the equilibrium state is achieved. The equilibrium time is the time required for attainment equilibrium state, and the pigment sorbed amount at equilibrium reveals the maximum sorption capacity of the sorbent below the same operating conditions. Fig. 3 illustrations the sorption of CV on AC in the existence of high ultrasound intensity. It can be observed that at lower sorption equilibrium pigment concentration, sorption capacity elevates sharply with the rise of equilibrium pigment concentration. The isotherm data is fitted to various sorption isotherm models to determine the best-fit equilibrium isotherms model for sorption CV (El-Sayed, 2011). Sorption data were used in describing by the isotherm models as Langmuir, Freundlich, D-R and Timken models. The Langmuir model that established on the supposition of a monolayer of solute on a homogenous surface with all sorption sites identical (Hassan and Aly, 2019). While the Freundlich model is an empirical expression assuming sorption on the heterogeneous surface and active sites that have different energies (Yakout et al., 2018). The values of parameters and  $R^2$  (correlation coefficients) determined by plotting for Freundlich ( $\log Q_e$  against  $\log C_e$ ) (Fig. 4), Langmuir ( $C_e/Q_e$  against  $C_e$ ) (Fig. 5), D-R ( $\ln Q_e$  against  $\epsilon^2$ ) (Fig. 6) and Timken ( $Q_e$  against  $\ln C_e$ ) (Fig. 7) are recorded in Table 2. As observed although the equilibrium data were fitted well to the Langmuir model and Freundlich model, the Langmuir model demonstrated more suitable to the sorption data than the Freundlich model. According to

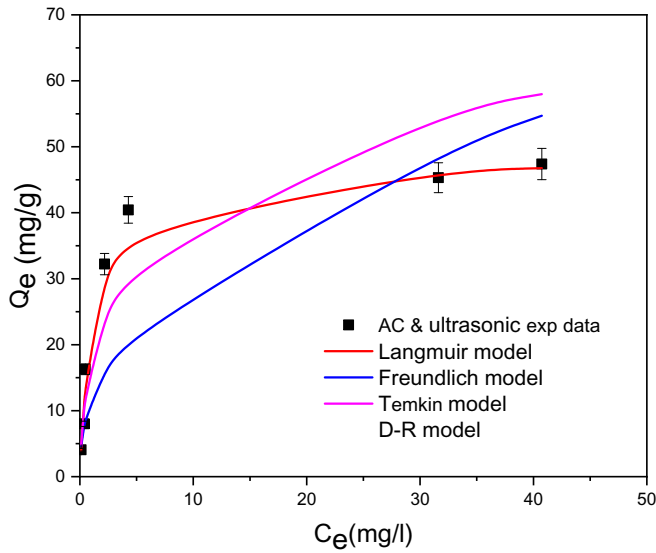


Fig. 3. Sorption isotherms of CV under high ultrasound intensity- Experimental data and non-linear fitting method.

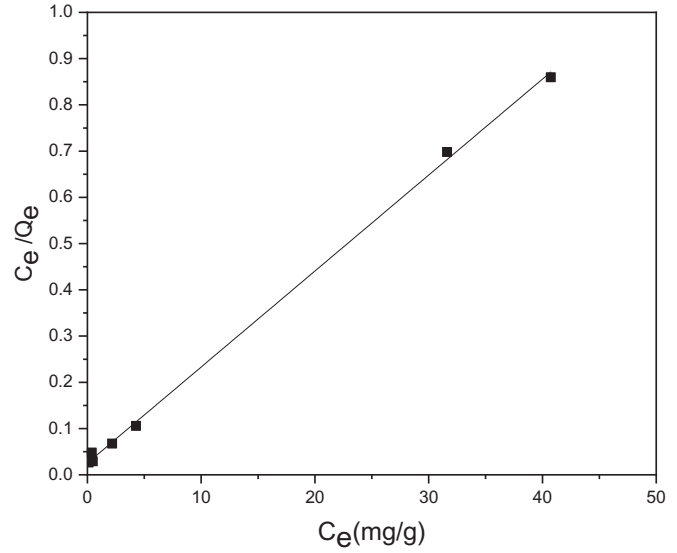


Fig. 5. Langmuir plot of CV sorption.

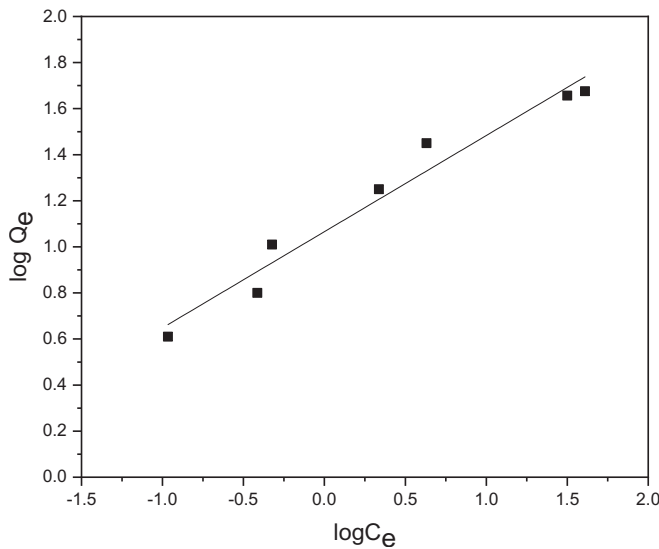


Fig. 4. Freundlich plot of CV sorption.

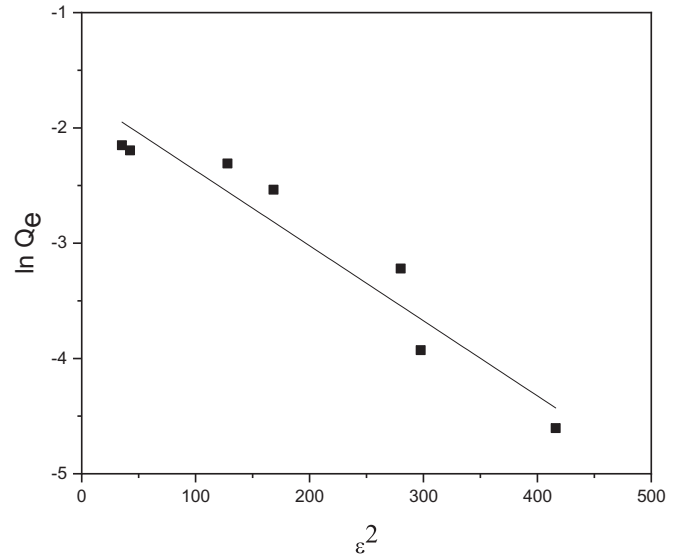


Fig. 6. D-R plot of CV sorption.

the Langmuir isotherm model, the maximum sorption capacity of AC for CV was obtained to be 50.1 mg/g. The Freundlich constant value,  $K_F$  signifies the degree of sorption. The  $n$  is an empirical parameter related to the heterogeneity of the sorbent surface. The higher the value of  $n$  indicates the stronger the sorption intensity. In general  $n > 1$  illustrates that sorbate is favorably sorbed on a sorbent, and in particular, the  $n$  value is significantly greater than unity. The constant of D–R isotherm model,  $K_{D-R}$  gave an idea about the sorption mean free energy ( $E$ ) and can be computed using equation (11) as follow (Gad et al., 2016):

$$E = \frac{1}{\sqrt{2K_{D-R}}} \quad (11)$$

The  $E$  magnitude can determine the type of sorption. The physical sorption occurs when  $E$  value is less 8 kJ/mol and the chemical ion exchange occur when  $E$  value more than 8 kJ/mol (Gad et al., 2016). The sorption means free energy for this study is less

than 8 kJ/mol. (Table 2), which indicates that the sorption of CV onto AC classified as a physical sorption process.

Temkin isotherm model supposes that the reduction of the sorption heat is linear and the process can describe via a uniform spreading of binding energies (Abd El-Magied et al., 2018).  $\beta$  is constant of the Temkin which can be computed using equation (12) as follow:

$$\beta = RT \frac{1}{b} \quad (12)$$

The  $\beta$  value of CV onto AC was found to be 7.75 kJ/mol which less than 20 kJ/mol, indicating that a sorption process with a physical sorption nature. The theoretical parameters of sorption isotherms with  $R^2$ , RMSE, SSE, and  $X^2$  are recorded in Table 2. It observed that the Langmuir isotherm model gives higher esteems of  $R^2$ , RMSE,  $X^2$  and SSE.

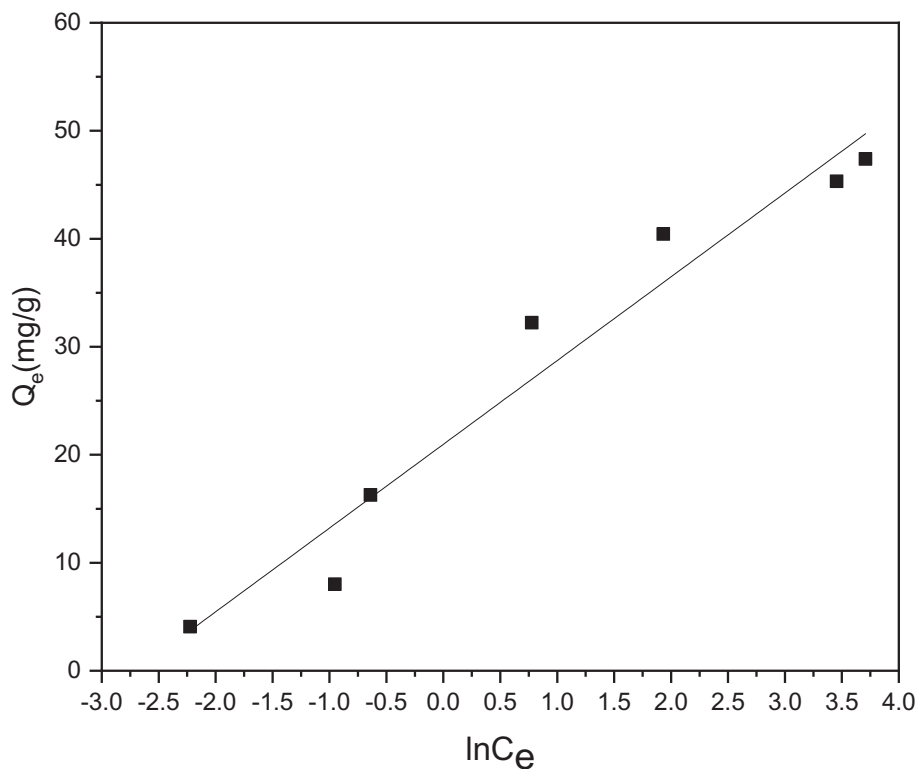


Fig. 7. Timken plot of CV sorption.

**Table 2**  
Isotherm parameters of CV sorption on AC under high-intensity ultrasound.

Model	parameters	value
Langmiur	$Q_{Lan}$ (mg/g)	50.1
	$K_L$ (L/mg)	3.298
	$R^2$	0.985
	RMSE	2.5
	SSE	4.7
	$\chi^2$	0.174
Freundlich	$K_F$ (mg/g) (L/mg) <sup>1/n</sup>	15.4
	$n$	4.5
	$R^2$	0.959
	RMSE	12.2
	SSE	107.6
	$\chi^2$	4.64
D-R	$Q_m$ (mg/g)	5.57
	$K_{D-R}$ (mol <sup>2</sup> /kJ <sup>2</sup> )	$9.51 \times 10^{-3}$
	$E$ (kJ/mol)	7.2
	$R^2$	0.90
	RMSE	8.68
	SSE	53.91
Timken	$\beta$ (kJ/mol)	7.75
	$K_T$ (L/g)	14.8
	$b$	316
	$R^2$	0.944
	RMSE	5.25
	SSE	19.7
	$\chi^2$	0.73

#### 4.5. Effect of temperature

Fig. 8 clearly demonstrates that the sorption capacity of AC under high-intensity ultrasound increase with different temperature (298, 338 and 353 K). Thermodynamic parameters, i.e. the free energy ( $\Delta G^0$ ), enthalpy ( $\Delta H^0$ ) and entropy ( $\Delta S^0$ ) are resolved from

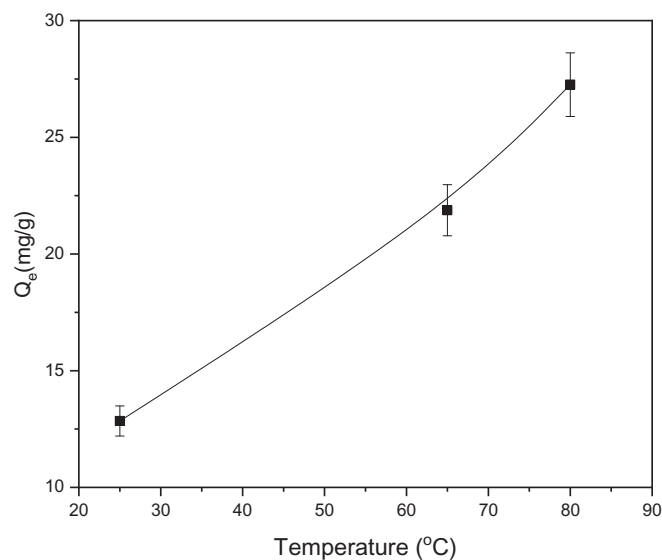


Fig. 8. Temperature effect on the sorption of CV on AC under high-intensity ultrasound.

the next equations (Abbas et al., 2014):

$$K_c = \frac{C_e}{C_o - C_e} \quad (13)$$

$$\Delta G^0 = -RT \ln K_c \quad (14)$$

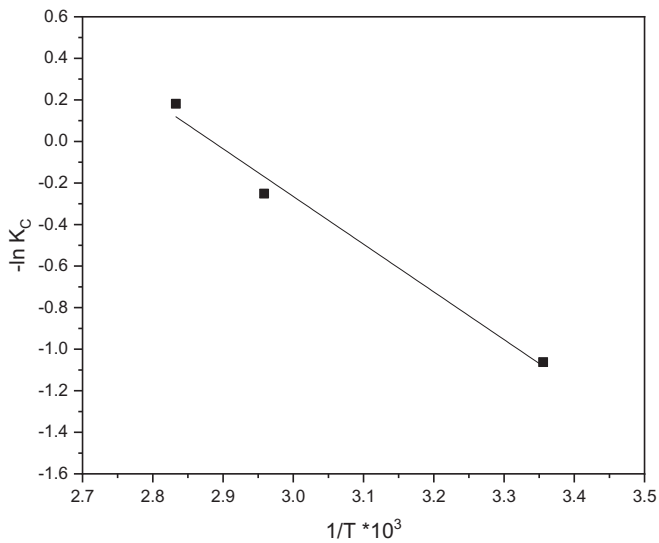


Fig. 9. Van't Hoff plot for the sorption of CV pigment.

$$\Delta G^{\circ} = \Delta H^{\circ} - T\Delta S^{\circ} \quad (15)$$

$$-\ln K_c = \left( \frac{\Delta H^{\circ}}{R} \right) \cdot \frac{1}{T} - \frac{\Delta S^{\circ}}{R} \quad (16)$$

Here  $K_c$  is the distribution constant,  $T$  is the absolute temperature in Kelvin,  $R$  is the gas constant,  $C_0$  (mg/L) is an initial concentration of CV and  $C_e$  (mg/L) is the concentration at equilibrium, and. The  $\Delta H^{\circ}$ ,  $\Delta S^{\circ}$  values acquired from the slope and intercept of the Van't Hoff plots of  $-\ln K_c$  against  $1/T$  (Fig. 9) and the  $\Delta G^{\circ}$  esteems at various temperatures are reported in Table 3. The negative values of  $\Delta G^{\circ}$  reflect that the sorption of CV onto AC under high-intensity ultrasound is feasible and spontaneous. It can be observed that the  $\Delta H^{\circ}$  value reported by Lin et al. (2008) is negative ( $-19.09$  kJ/mol), demonstrating that the sorption process onto AC was found to be the exothermic.

Table 3

Equilibrium constant and thermodynamic parameters for the sorption of CV pigment onto AC under high-intensity ultrasound.

T (K)	$C_e$ (mg/L)	$Q_e$ (mg/L)	$K_c$	$1/T$ ( $k^{-1}$ )	$-\ln K_c$	$\Delta G^{\circ}$ kJmol <sup>-1</sup>	$\Delta H^{\circ}$ kJmol <sup>-1</sup>	$\Delta S^{\circ}$ Jmol <sup>-1</sup> K <sup>-1</sup>
298	74.30	12.84	2.892	$3.35 \times 10^{-3}$	-1.06	-2.631		
338	56.25	21.87	1.28	$2.95 \times 10^{-3}$	-0.25	-0.706	-19.09	55.73
353	45.48	27.25	0.8	$2.83 \times 10^{-3}$	0.18	0.531		

Table 4

Comparison of the sorption of CV by different methods and sorbents.

Sorbents	Methods	Maximum capacity (mg/g)	Ref.
peanut husk powder	Sono-sorption	—	Low et al. (2018)
Artocarpus heterophyllus (jackfruit) leaf powder	Biosorption	43.39	Saha et al. (2012)
FeGAC/H <sub>2</sub> O <sub>2</sub>	Ultrasound/heterogeneous	—	Zhang et al. (2013)
CaFe <sub>2</sub> O <sub>4</sub> -NPs	Magnetic stirrer	10.67	An et al. (2015)
CuO@AC and CeO <sub>2</sub> -CuO@AC catalysts	Microwave catalytic oxidation	—	Yin et al. (2016)
Soil-Silver Nanocomposite (soil-AgNP)	Magnetic stirrer	1.918	Satapathy and Das (2014)
Raw Tunisian Smectite Clay	Sono-sorption	86.543	Hamza et al. (2018)
zinc (II) oxide nanorods loaded on activated carbon	Sono-sorption	81.64	Dil et al. (2017)
Activated carbon	Sono-sorption	35.64	Dil et al. (2017)
AC	Sono-sorption	50.1	This work

#### 4.6. Comparison with other sorbents

Table 4. The maximum capacity ( $Q_{lan}$ ) obtained by Langmuir isotherm for CV pigment sorption was 50.1 mg/g for ultrasonic assisted simultaneous sorption, which indicates the applicability of AC sorbent for treatment of real wastewater containing a high amount of understudy CV and also indicates the superiority of AC sorbent in comparison to previously reported material. The good performance of this work supports the ultrasound unique role to enhance the mass transfer process and the affinity between pigment and sorbent (Asfaram et al., 2016). In addition, the performance comparison of ultrasound-assisted with other methods establishes that ultrasound is an effective and promising technology to sorption of pigment from laden aqueous solutions.

However, this study has been limited in the laboratory scale because of the lack of industrial scale ultrasonic equipment. Ultrasonic equipment still suffers from the high cost and the limitation of power dissipation to the reactor. By developing better ultrasonic transducer technology and more effectively converting electrical energy to acoustic energy, textile dyebath effluents can be decolorized and mineralized with large-scale ultrasonic treatment before being discharged into the main effluent. Ultrasonically pretreated dyebath effluents can also be recycled in the plant to prevent excessive water usage by the industry or discharge for biological treatment. But, there are still some limitations to apply this combined system to the dyebath effluents because they contain a lot of auxiliary chemicals and other dye components rather than as a single dyestuff.

Alternatively, cost analysis is needed to assess on the cost-effectiveness of utilizing combined ultrasound and AC for pigment decolorization. It is predictable that the optimization results obtainable from this study may be responsible for background data for removal of pigments to improve researches in future.

## 5. Conclusion

Removal of CV was examined under ultrasound and combined ultrasound/AC. Ultrasound or AC alone were insufficient for removal dye color. Then, combined ultrasound/AC was applied to remove dye color. The decolorization efficiency is much higher in the presence of combined ultrasound/AC than using ultrasound alone or AC alone. So, the sono-sorption technique significantly enhanced CV removal onto AC. The experimental results show that

sono-sorption of CV was influenced by the several parameters for instance initial concentration and temperature. The sorption CV onto AC demonstrated more suitable for Langmuir than the Freundlich isotherm model. The maximum monolayer sorption capacity was 50.1 mg/g. The nature of CV sorption on AC was physical sorption. The enthalpy and free energy indicate an exothermic, feasible and spontaneous process. In summary, the combination of the ultrasound and sorption process as an environmentally friendly, a cost-effective, easily operating and promising technique was operated for the CV removal from wastewater.

## Acknowledgments

The authors extend their appreciation to the Deanship of Scientific Research at King Saud University for funding this work through research group No. RG-1436-026.

## References

- Abbas, M., Aksil, T., Trari, M., 2018. Removal of toxic methyl green (MG) in aqueous solutions by apricot stone activated carbon-equilibrium and isotherms modeling. *Desalination Water. Treat.* 125, 93–101.
- Abbas, M., Kaddour, S., Trari, M., 2014. Kinetic and equilibrium studies of cobalt adsorption on apricot stone activated carbon. *J. Ind. Eng. Chem.* 20 (3), 745–751.
- Abd El-Magied, M.O., Hassan, A.M.A., Gad, H.M.H., Mohammed, T.F., Youssef, M.A.M., 2018. Removal of nickel (II) ions from aqueous solutions using modified activated carbon: a kinetic and equilibrium study. *J. Dispersion Sci. Technol.* 39 (6), 862–873.
- An, S., Liu, X., Yang, L., Zhang, L., 2015. Enhancement removal of crystal violet dye using magnetic calcium ferrite nanoparticle: study in single- and binary-solute systems. *Chem. Eng. Res. Des.* 94, 726–735.
- Asfaram, A., Ghaedi, M., Hajati, S., Goudarzi, A., 2016. Synthesis of magnetic  $\gamma$ - $\text{Fe}_2\text{O}_3$ -based nanomaterial for ultrasonic assisted dyes adsorption: modeling and optimization. *Ultrason. Sonochem.* 32, 418–431.
- Cheng, Y., Lin, H., Chen, Z., Megharaj, M., Naidu, R., 2012. Biodegradation of crystal violet using *Burkholderia vietnamiensis* C09V immobilized on PVA–sodium alginate–kaolin gel beads. *Ecotoxicol. Environ. Saf.* 83, 108–114.
- Cohen-Ofri, I., Weiner, L., Boaretto, E., Mintz, G., Weiner, S., 2006. Modern and fossil charcoal: aspects of structure and diagenesis. *J. Archaeol. Sci.* 33 (3), 428–439.
- Dastkhooon, M., Ghaedi, M., Asfaram, A., Goudarzi, A., Mohammadi, S.M., Wang, S., 2017. Improved adsorption performance of nanostructured composite by ultrasonic wave: optimization through response surface methodology, isotherm and kinetic studies. *Ultrason. Sonochem.* 37, 94–105.
- Devi, A.P., Mishra, P.M., 2019. Biosorption of dysprosium (III) using raw and surface-modified bark powder of *Mangifera indica*: isotherm, kinetic and thermodynamic studies. *Environ. Sci. Pollut. Res.* 26 (7), 6545–6556.
- Dil, E.A., Ghaedi, M., Asfaram, A., 2017. The performance of nanorods material as adsorbent for removal of azo dyes and heavy metal ions: application of ultrasound wave, optimization and modeling. *Ultrason. Sonochem.* 34, 792–802.
- El-Sayed, G.O., 2011. Removal of methylene blue and crystal violet from aqueous solutions by palm kernel fiber. *Desalination* 272 (1), 225–232.
- Entezari, M.H., Bastami, T.R., 2008. Influence of ultrasound on cadmium ion removal by sorption process. *Ultrason. Sonochem.* 15 (4), 428–432.
- Entezari, M.H., Keshavarzi, A., 2001. Phase-transfer catalysis and ultrasonic waves II: saponification of vegetable oil. *Ultrason. Sonochem.* 8 (3), 213–216.
- Entezari, M.H., Soltani, T., 2009. Cadmium and lead ions can be removed simultaneously from a binary aqueous solution by the sono-sorption method. *Ultrason. Sonochem.* 16 (4), 495–501.
- Eren, Z., 2012. Ultrasound as a basic and auxiliary process for dye remediation: a review. *J. Environ. Manag.* 104, 127–141.
- Gad, H., Omar, H., Aziz, M., Hassan, M., Khalil, M., 2016. Treatment of rice husk ash to improve adsorption capacity of cobalt from aqueous solution. *Asian J. Chem.* 28 (2), 385.
- Gupta, V.K., Jain, R., Varshney, S., 2007. Electrochemical removal of the hazardous dye Reactofix Red 3 BFN from industrial effluents. *J. Colloid Interface Sci.* 312 (2), 292–296.
- Hamza, W., Dammak, N., Hadjtaief, H.B., Eloussaief, M., Benzina, M., 2018. Sono-assisted adsorption of crystal violet dye onto Tunisian smectite Clay: characterization, kinetics and adsorption isotherms. *Ecotoxicol. Environ. Saf.* 163, 365–371.
- Harrache, Z., Abbas, M., Aksil, T., Trari, M., 2019. Thermodynamic and kinetics studies on adsorption of Indigo Carmine from aqueous solution by activated carbon. *Microchem. J.* 144, 180–189.
- Hassan, M.R., Aly, M.I., 2019. Adsorptive removal of cesium ions from aqueous solutions using synthesized Prussian blue/magnetic cobalt ferrite nanoparticles. *Part. Sci. Technol.* 1–11.
- Jain, R., Gupta, V.K., Sikarwar, S., 2010. Adsorption and desorption studies on hazardous dye Naphthol Yellow S. *J. Hazard Mater.* 182 (1), 749–756.
- Kim, T.-H., Park, C., Yang, J., Kim, S., 2004. Comparison of disperse and reactive dye removals by chemical coagulation and Fenton oxidation. *J. Hazard Mater.* 112 (1), 95–103.
- Lin, J.X., Zhan, S.L., Fang, M.H., Qian, X.Q., Yang, H., 2008. Adsorption of basic dye from aqueous solution onto fly ash. *J. Environ. Manag.* 87 (1), 193–200.
- Liu, W., Zhang, J., Cheng, C., Tian, G., Zhang, C., 2011. Ultrasonic-assisted sodium hypochlorite oxidation of activated carbons for enhanced removal of Co(II) from aqueous solutions. *Chem. Eng. J.* 175, 24–32.
- Low, S.K., Tan, M.C., Chin, N.L., 2018. Effect of ultrasound pre-treatment on adsorbent in dye adsorption compared with ultrasound simultaneous adsorption. *Ultrason. Sonochem.* 48, 64–70.
- Majewska-Nowak, K., Winnicki, T., Wiśniewski, J., 1989. Effect of flow conditions on ultrafiltration efficiency of dye solutions and textile effluents. *Desalination* 71 (2), 127–135.
- Mardoyan, A., Braun, P., 2015. Analysis of Czech subsidies for solid biofuels. *Int. J. Green Energy* 12 (4), 405–408.
- Maroušek, J., Stehel, V., Vochozka, M., Kolář, L., Maroušková, A., Strunecký, O., Peterka, J., Kopecký, M., Shreedhar, S., 2019. Ferrous sludge from water clarification: changes in waste management practices advisable. *J. Clean. Prod.* 218, 459–464.
- Maroušek, J., Zeman, R., Vaníčková, R., Hašková, S., 2014. New concept of urban green management. *Clean Technol. Environ. Policy* 16 (8), 1835–1838.
- Mullerova, S., Baldikova, E., Prochazkova, J., Pospiskova, K., Safarik, I., 2019. Magnetically modified macroalgae *Cymopolia barbata* biomass as an adsorbent for safranin O removal. *Mater. Chem. Phys.* 225, 174–180.
- Muthukumar, M., Sargunamani, D., Selvakumar, N., Venkata Rao, J., 2004. Optimization of ozone treatment for colour and COD removal of acid dye effluent using central composite design experiment. *Dyes Pigments* 63 (2), 127–134.
- Pathania, D., Sharma, S., Singh, P., 2017. Removal of methylene blue by adsorption onto activated carbon developed from *Ficus carica* bast. *Arabian J. Chem.* 10, S1445–S1451.
- Rodrigues, E., Almeida, O., Brasil, H., Moraes, D., dos Reis, M.A.L., 2019. Adsorption of chromium (VI) on hydroxalite-hydroxyapatite material doped with carbon nanotubes: equilibrium, kinetic and thermodynamic study. *Appl. Clay Sci.* 172, 57–64.
- Saha, P.D., Chakraborty, S., Chowdhury, S., 2012. Batch and continuous (fixed-bed column) biosorption of crystal violet by *Artocarpus heterophyllus* (jackfruit) leaf powder. *Colloids Surfaces B Biointerfaces* 92, 262–270.
- Satapathy, M.K., Das, P., 2014. Optimization of crystal violet dye removal using novel soil-silver nanocomposite as nanoadsorbent using response surface methodology. *J. Environ. Chem. Eng.* 2 (1), 708–714.
- Şayan, E., 2006. Optimization and modeling of decolorization and COD reduction of reactive dye solutions by ultrasound-assisted adsorption. *Chem. Eng. J.* 119 (2), 175–181.
- Shirsath, S.R., Patil, A.P., Bhanvase, B.A., Sonawane, S.H., 2015. Ultrasonically prepared poly(acrylamide)-kaolin composite hydrogel for removal of crystal violet dye from wastewater. *J. Environ. Chem. Eng.* 3 (2), 1152–1162.
- Sun, D., Zhang, X., Wu, Y., Liu, X., 2010. Adsorption of anionic dyes from aqueous solution on fly ash. *J. Hazard Mater.* 181 (1), 335–342.
- Thompson, L.H., Doraiswamy, L.K., 1999. Sonochemistry: science and engineering. *Ind. Eng. Chem. Res.* 38 (4), 1215–1249.
- Yakout, S.M., Hassan, M.R., Aly, M.I., 2018. Synthesis of magnetic alginate beads based on magnesium ferrite ( $\text{MgFe}_2\text{O}_4$ ) nanoparticles for removal of Sr (II) from aqueous solution: kinetic, equilibrium and thermodynamic studies. *Water Sci. Technol.* 77 (11), 2714–2722.
- Ye, C., Wang, Q., Luo, Z., Xie, G., Jin, K., Siyil, M., Cen, K., 2017. Characteristics of coal partial gasification on a circulating fluidized bed reactor. *Energy Fuels* 31 (3), 2557–2564.
- Yin, J., Cai, J., Yin, C., Gao, L., Zhou, J., 2016. Degradation performance of crystal violet over  $\text{CuO}/\text{AC}$  and  $\text{CeO}_2\text{-CuO}/\text{AC}$  catalysts using microwave catalytic oxidation degradation method. *J. Environ. Chem. Eng.* 4 (1), 958–964.
- Zhang, H., Gao, H., Cai, C., Zhang, C., Chen, L., 2013. Decolorization of crystal violet by ultrasound/heterogeneous fenton process. *Water Sci. Technol.* 68 (11), 2515–2520.
- Zhao, Y., Cho, C.-W., Cui, L., Wei, W., Cai, J., Wu, G., Yun, Y.-S., 2018. Adsorptive removal of endocrine-disrupting compounds and a pharmaceutical using activated charcoal from aqueous solution: kinetics, equilibrium, and mechanism studies. *Environ. Sci. Pollut. Res.*